phys. stat. sol. (a) **200**, No. 2, 378–387 (2003) / **DOI** 10.1002/pssa.200306689

Non-adiabatic small polaron hopping conduction in sodium borate tungstate glasses

A. Al-Shahrani[1], **A. Al-Hajry**[1], and **M. M. El-Desoky**[*, 2]

[1] Physics Department, College of Science, King Khalid University, PO Box 9004, Abha, Saudi Arabia
[2] Physics Department, Faculty of Education, Suez Canal University, El-Arish, Egypt

Received 8 April 2003, revised 21 August 2003, accepted 25 August 2003
Published online 14 November 2003

PACS 71.38.Ht, 72.20.Ee, 72.80.Ng

The dc electrical conductivity of $(100–x)Na_2B_4O_7–xWO_3$ (x = 5, 15, 20 and 30 mol%) glasses is reported in the temperature range 323–473 K. The density and molar volume for these glasses are consistent with the ionic size, atomic weight and amount of different elements in the glasses. At high temperatures the Mott model of phonon-assisted small polaron hopping between nearest neighbours is consistent with conductivity data, while at intermediate temperatures the Greaves variable-range hopping model is found to be appropriate. The estimated model parameters such as number of ions per unit volume, hopping distance, polaron radius and activation energy are found to be consistent with the formation of localized states in these glasses. The electrical conduction of these glasses is confirmed to be that of non-adiabatic small polaron hopping.

1 Introduction

For some years glasses containing transition metal oxides (TMOs) have attracted attention because of their potential applications in electrochemical, electronic and electro-optical devices [1–4]. TMOs, for instance WO_3 or V_2O_5, when mixed with glass formers like B_2O_3, P_2O_5 and SiO_2 form stable glasses in a comparatively wide range of compositions. A general condition for the semiconducting behaviour is the ability of transition metal ions to coexist in more than one valance state, for instance W^{5+} and W^{6+}, so that the conduction can take place by transfer of electrons from a low- to a high-valance state. The charge transport at high temperature ($T > \theta_D/2$, where T is the absolute temperature and θ_D is the Debye temperature) in these glasses is usually considered in terms of the small polaron hopping (SPH) model [5–8]. On the other hand, at low temperature ($T < \theta_D/4$) the conduction is interpreted by variable-range hopping (VRH) [9, 10]. The charge carrier concentrations are related to the amounts of TMO and to the ratio of reduced ions (W^{5+}) to the total quantity of TMO.

The theoretical considerations of small polaron hopping are based on the molecular crystal model introduced by Holstein [11]. This model was extended to disordered systems by Schnakenberg [12] and Emin [13]. The main feature of the electrical conductivity in TMO glasses is that the activation energy decreases with decreasing temperature. As the temperature is lowered the multiphonon processes are frozen out and the high-temperature activation energy is expected to decrease continuously from $W_H + W_D/2$ to W_D, where W_H is the polaron hopping energy and W_D is a disorder term arising from the energy differences of neighbouring hopping sites. In the temperature range $T < \theta_D/4$ charge carrier transport should be an acoustic phonon-associated hopping process and in the low-temperature limit the activation energy for a hop upward in energy is W_D. In the high-temperature range ($T > \theta_D/2$) a multiphonon proc-

[*] Corresponding author: e-mail: mmdesoky@yahoo.com, Phone: +2024529840, Fax: +2068350065

ess takes place and the activation energy for small polaron hop upwards in energy by an amount W_D is $W_H + W_D/2$ regardless of whether the phonons involved are acoustic, optical or mixed optical and acoustic [14, 15].

In the present work, we report the conductivity and density of WO_3–$Na_2B_4O_7$ type glassy systems. These also show some interesting features along with decreasing effect on conductivity with increase in tungsten content. The main objective of this work is to discuss the mechanism of electrical conduction for WO_3–$Na_2B_4O_7$ glasses.

2 Experimental

The WO_3–$Na_2B_4O_7$ glasses were prepared from analar grade chemicals by making up appropriate molar compositions. Appropriate amounts of the different chemicals as powders were weighed on a K-Roy monopan balance. The homogeneous mixture was added to a platinum crucible and placed in a furnace. Melting was carried out under controlled conditions at temperatures ranging from 1100 to 1200 ± 5 °C for 1 h with occasional stirring. The melt was then poured onto a polished copper block kept at room temperature and was immediately pressed by a similar copper block. For electrical measurements, disc-shaped samples of ~10 mm diameter were cut and polished with very fine lapping papers. Silver paste electrodes were deposited on both faces of these polished samples. The dc conductivity of the samples was measured using a Keithley 485 electrometer, in the range 323–473 K. A Levell Tester TM14 was used for the direct measurement of resistance over the temperature range 340–420 K. The *I*–*V* characteristics between the electrodes were verified. The densities of glass samples were measured using the Archimedes principle. The accuracy in the measurement of density was ±0.001 g/cm^3. The total number of transition metal ions was determined from the composition of the glasses.

To check the amorphous nature of the glass samples, X-ray diffraction (XRD) patterns were obtained using a Philips Analytical X-ray BV type PW 1840 instrument. It was observed that all the samples were amorphous in nature.

3 Results and discussion

3.1 Density

The density, *d*, and molar volume, V_m, for the glass samples are shown in Fig. 1. These properties change linearly as a function of glass composition. The density results show that as the tungsten cation concentration increases the glass structure becomes less open, allowing for the probable formation of a decreas

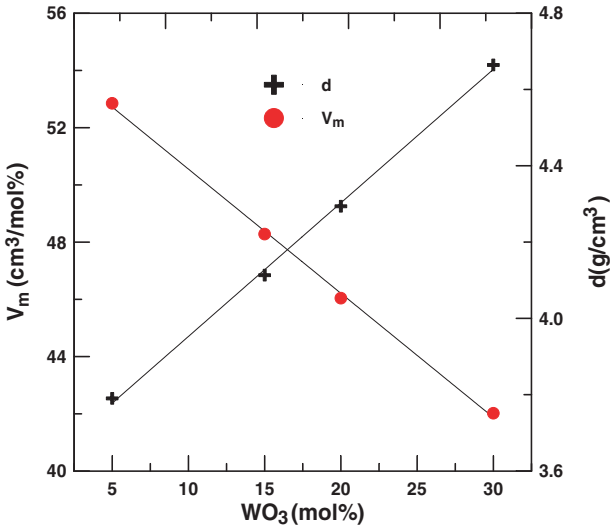

Fig. 1 (online colour at: www.interscience.wiley.com) Effect of WO_3 content on density, *d*, and molar volume, V_m, for different glass compositions.

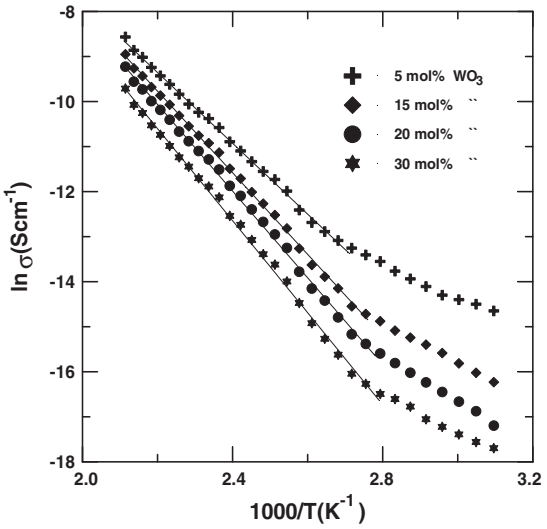

Fig. 2 Temperature dependence of dc conductivity, σ, for different glass compositions. The solid lines are calculated using the least-squares technique.

ing number of non-bridging oxygens (NBOs) [16]. Also, from Fig. 1 it is seen that the molar volume decreases with increasing tungsten content; this may be due to the effect of the polarizing power strength (PPS), which is a measure of the ratio of the cation valance to its diameter. The PPS of the tungsten cation is smaller than that of the boron cation, which causes the packing fraction to consequently increase due to the weak attracting force of tungsten cations to oxygen anions. In the present glass system the densities vary from 3.79 to 4.66 g/cm^3 revealing a linear relationship with an obvious systematic trend as a function of tungsten content. Here the composition dependence of molar volume gives information about the coordination state of the tungsten cations. The observed decrease of molar volume suggests that most boron cations have on average a large coordination number of boron atoms leading to an increase of molar volume [16, 17]. The density and molar volume for these glasses are consistent with the ionic size, atomic weight and amount of different elements in the glasses [7].

3.2 Dc conductivity and activation energy

Figure 2 shows dc conductivity, σ, as a function of inverse temperature for the various glass compositions under study. It is observed that σ increases smoothly with increasing temperature, indicating a temperature-dependent activation energy, W, characteristic of a SPH conduction mechanism in TMO glasses [3, 9]. The experimental conductivity data in such a situation are well described with an activation energy for conduction, W, given by the Mott formula [18, 19]

$$\sigma = (\sigma_0/T)\ \exp(-W/kT)\,, \tag{1}$$

where σ_0 is a pre-exponential factor as discussed below. Values of W obtained from fitting of the linear part of the curves in Fig. 2 (high-temperature region) are given in Table 1. Figure 2 also shows the devia-

Table 1 Chemical composition and physical properties of WO_3–$Na_2B_4O_7$ glasses.

glass no.	nominal composition (mol%)		$W \pm 0.004$ (eV)	$V_m \pm 0.1$ (cm^3/mol)	$N \pm 0.02$ ($\times 10^{22}$/cm^3)	$R \pm 0.02$ (Å)	$\theta_D \pm 1$ (K)	$\nu_0 \pm 0.01$ ($\times 10^{13}$/s)
	WO_3	$Na_2B_4O_7$						
1	5	95	0.69	52.85	1.18	4.39	740	1.54
2	15	85	0.80	48.28	1.29	4.26	726	1.51
3	20	80	0.85	46.04	1.35	4.19	720	1.50
4	30	70	0.91	42.02	1.48	4.07	718	1.49

tion from a linear plot occurs around $\theta_D/2$ (Table 1). In the low-temperature region ($T < \theta_D/2$) the conduction is attributed to being electronic, while in the high-temperature region ($T > \theta_D/2$) Na^+ ions may become mobile and contribute to the conduction process [3, 4]. In TMO glasses with mobile cations different conduction processes contribute to electric conduction at different temperature ranges leading to different values of activation energy [7, 20].

To obtain evidence for the nature of these two types of conduction, the time effect of 40 V on the electrical resistance of the glass samples at $T = 340$ and 420 K has been studied over a period of 2 h. The resistance at $T = 340$ K ($<\theta_D/2$) for the glass samples is found to be constant, whereas that at $T = 420$ K ($>\theta_D/2$) increases exponentially by an order of magnitude. This indicates that the conduction at $T < \theta_D/2$ my be electronic, while at $T > \theta_D/2$ Na^+ ions may become mobile and contribute to the conduction process [3].

The logarithm of the conductivity (Fig. 2) shows a linear temperature dependence up to a critical temperature T_D ($\theta_D/2$) and then the slope changes with a deviation from linearity and the activation energy is temperature dependent. Such a behaviour is a feature of SPH [1, 6, 21]. So we first discuss the thermal variation of conductivity assuming the SPH model [2, 6] based on a strong coupling of electrons with the lattice by a single phonon. This model gives σ in the non-adiabatic regime for TMO glasses from Eq. (1) as

$$\sigma = \frac{\nu_0 N e^2 R^2}{kT} C(1-C) \exp(-2\alpha R) \exp\left(\frac{-W}{kT}\right). \tag{2}$$

The activation energy, W, can be written as

$$W = W_H + W_D/2 \quad (\text{for } T > \theta_D/2), \tag{3a}$$

$$W = W_D \quad (\text{for } T < \theta_D/4). \tag{3b}$$

The pre-exponential factor, σ_0, in Eq. (1) is given by

$$\sigma_0 = \nu_0 N e^2 R^2 C(1-C) \exp(-2\alpha R)/kT, \tag{4}$$

where ν_0 is the optical phonon frequency (generally $\nu_0 \approx 10^{13}$/s [22, 23]), N the transition metal density, C the fraction of reduced transition metal ion ($C = W^{5+}/W_{total}$), α the tunnelling factor (the ratio of wave function decay), R the hopping distance or W–W ion spacing, W_H the hopping energy and W_D the disorder energy defined as the difference of electronic energies between two hopping sites [24].

Figure 3 shows the plot of activation energy and electrical conductivity at different temperatures (410, 440 and 470 K) as a function of WO_3 content. It is observed that as the percentage of WO_3 increases the activation energy of electrical conduction increases and electrical conductivity decreases, in a linear manner. This is consistent qualitatively with Eq. (2) proposed for polaron hopping at high temperatures. The high value of activation energy and low value of electrical conductivity are similar to those for $Na_2P_2O_6$–Fe_2O_3 and Fe_2O_3–Bi_2O_3–B_2O_3 glasses [17, 25]. This change in conductivity and activation energy may help to detect the structural changes as a consequence of increasing WO_3 and decreasing sodium oxide content. Generally, it is known that addition of tungsten oxide to the glass decreases the ionic conductivity as a result of increasing bridging oxygen ions. This may decrease the open structure (i.e. the non-bridging oxygen ions) through which the charge carriers can move with lower mobility. On the other hand, this result provides the reason why the coulombic binding force of the sodium ion is affected by the type of transition metal ion (TMI) that is located at a neighbouring site. The change in the binding force may cause the change in the sodium ion mobility, due to the large difference in ionic sizes of Na and W, leading to smaller values of mobility and an increase of stability and decrease of conductivity [3, 26].

In the adiabatic hopping regime, however, αR in Eq. (2) becomes negligible [23, 24]; the conductivity, σ, and the pre-exponential factor, σ_0, in Eq. (2) are then expressed by the following equations [7, 8]:

$$\sigma = \frac{\nu_0 N e^2 R^2}{kT} C(1-C) \exp\left(\frac{-W}{kT}\right) \tag{5}$$

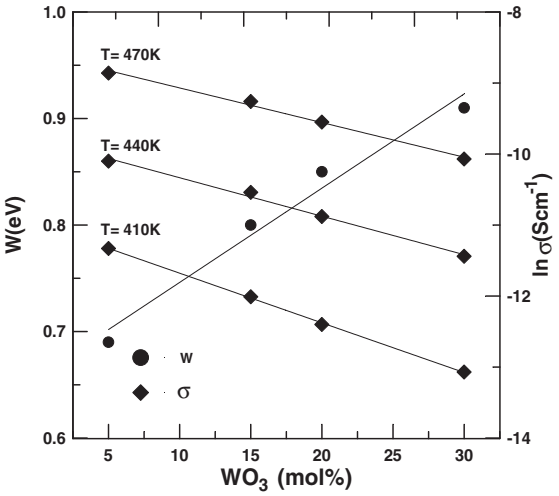

Fig. 3 Effect of WO_3 content on dc conductivity, σ, and activation energy, W, for different glass compositions.

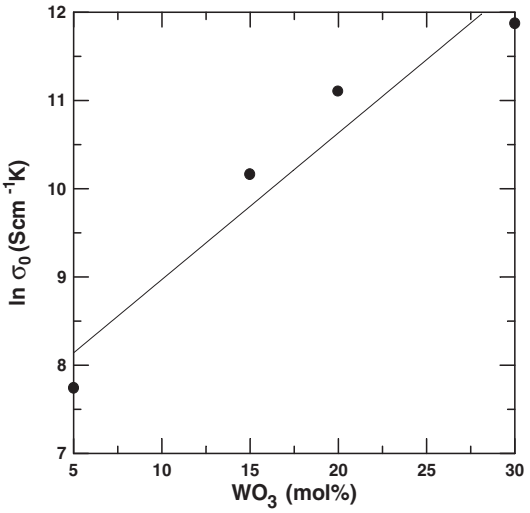

Fig. 4 Effect of WO_3 content on pre-exponential factor, σ_0, for different glass compositions.

and

$$\sigma_0 = \nu_0 N e^2 R^2 C(1 - C)/kT \,. \tag{6}$$

For adiabatic hopping the term σ_0 in Eq. (1) is not dependent on WO_3 concentration, and hardly varies [27, 28]. Therefore the dominant factor contributing to the conductivity should be W in the adiabatic regime [27, 28]. Figure 4 shows the effect of WO_3 concentration on σ_0, indicating an increase in σ_0 with WO_3 concentration from 5 to 30 mol%. From this result we conclude that the conduction in the glasses under study to be due to non-adiabatic hopping of polarons [29].

We estimate the optical phonon frequency, ν_0, in Eq. (4) using the experimental data from Table 1, according to $k\theta_D = h\nu_0$ (where h is Planck's constant) [22, 27]. To determine ν_0 for the different compositions the Debye temperature θ_D was estimated by $T > \theta_D/2$ (Eq. (3a)). θ_D of the present glasses was obtained to be 718–740 K, which is nearly the same as the values for V_2O_5–P_2O_5 glasses [30] and alkaline silicate glasses [31]. Thus, these estimated θ_D values are physically reasonable. Then, with the θ_D values obtained, ν_0 was calculated using $\nu_0 = k\theta_D/h$. The values of θ_D and ν_0 are summarized in Table 1.

3.3 Relation between activation energy for conduction and W–W ion spacing

The activation energies for electrical conduction, W, at temperatures between 355 and 473 K were found to be W = 0.69–0.91 eV (Table 1) for the present glasses. In our previous reports, we obtained W = 0.53–0.65 eV for CoO–$Na_2B_4O_7$ glasses [19], W = 0.53–0.96 eV for Fe_2O_3–WO_3–$Na_2B_4O_7$ glasses [32] and W = 0.33–0.89 eV for V_2O_5–BaO–B_2O_3 glasses [4]. The values for the present glass nearly agree with those for these glasses. The activation energy values for the WO_3–P_2O_5 [33] system were found to be much smaller than those for the present system. This difference is considered to be caused by differences in glass structure [3, 32, 34]. Furthermore, W depends on the W–W ion spacing, R, for the glasses containing TMO [24, 35, 36]. These results suggest that the electrical conduction is due to SPH between W–W ions [24, 35, 36].

In order to confirm the relation between W and R, the W ion density, N, was calculated using the following equation [37]:

$$N = 2\left(\frac{dWt_{WO_3}}{MW_{WO_3}}\right)N_A \,, \tag{7}$$

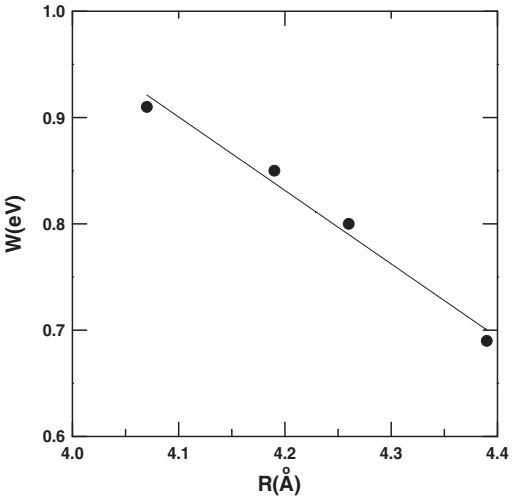

Fig. 5 Effect of W–W ion spacing, R, on activation energy, W, for different glass compositions.

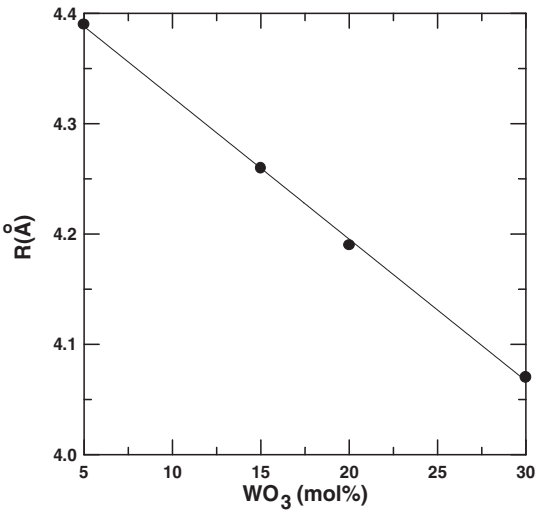

Fig. 6 Effect of WO_3 content on W–W ion spacing, R, for different glass compositions.

where d is the density, Wt_{WO_3} is the weight fraction of WO_3, MW_{WO_3} is the molecular weight of WO_3 and N_A is the Avogadro number. The relationship between N and R is generally described as

$$R = (1/N)^{1/3} . \tag{8}$$

The calculated values of N and R are summarized in Table 1.

The relation between the activation energy and the mean distance, R, between tungsten ions is illustrated in Fig. 5. In the range of measurements, W depends on the site-to-site distance R. This result shows that there is a prominent positive correlation between W and R between transition metal ions. This agrees with the results suggested by Sayer and Mansingh [38], Killias [39] and Austin and Garbet [40] delineating the dependence of W on the W–O–W site distance.

3.4 Small polaron hopping parameters

The polaron hopping energy, W_H, can be calculated from theory [41] and is given by

$$W_H = \frac{e^2}{4\varepsilon_P}\left(\frac{1}{r_P} - \frac{1}{R}\right) , \tag{9}$$

where

$$\frac{1}{\varepsilon_P} = \frac{1}{\varepsilon_\infty} - \frac{1}{\varepsilon_S} , \tag{10}$$

Table 2 Polaron hopping parameters of WO_3–$Na_2B_4O_7$ glasses.

glass no.	$W_H \pm 0.0002$ (eV)	$\varepsilon_P \pm 0.02$	$r_P \pm 0.001$ (Å)	$J \pm 0.0002$ (eV)	$N(E_F)$ ($\times 10^{21}$/(eV cm^3))	$A \pm 0.002$ (nm)	$\gamma_P \pm 0.002$
1	0.0062	24.51	1.77	0.0154	4.09	4.56	0.190
2	0.0076	20.35	1.72	0.0159	3.86	5.02	0.244
3	0.0092	17.21	1.69	0.0166	3.81	5.38	0.298
4	0.0110	15.50	1.64	0.0174	3.89	6.51	0.359

in which ε_S and ε_∞ are the static and high-frequency dielectric constants of the glass and r_P is the polaron radius. Usually it is appropriate to take $\varepsilon_P = \varepsilon_\infty$. These relations imply that the polaron should decrease in size as the number of sites increases. An approximate estimate of r_P was given by Bogomolov et al. [42] as

$$r_P = \frac{1}{2}\left(\frac{\pi}{6N}\right)^{1/3} = \frac{R}{2}\left(\frac{\pi}{6}\right)^{1/3} . \tag{11}$$

Here we regard R as the W–W ion spacing calculated from Eq. (8) on the basis of the glass densities measured. The W–W ion spacing, R, evaluated as 4.07–4.39 Å decreases with increasing WO_3 content (Fig. 6). The estimated values of r_P from Eq. (11), R and N are given in Table 1. An estimate of W_H can be made from Eq. (9) from the known values of R, r_P and ε_P. Values of ε_P were estimated from the Cole–Cole plot [43] and are given in Table 2, together with the calculated values of W_H. According to Eq. (3a) the difference existing between W and W_H arises from the disordering term $W_D/2$. An evaluation of $W_D/2$ from the theory of Miller and Abrahams [44] gives $W_D/2 = 0.05$ eV. It can be seen from Tables 1 and 2 that W and W_H values are much higher than the theoretically calculated values of $W_D/2$. The observed discrepancy is attributed to the existence of two possible coordinations for the tungsten ions in the glass [4, 40]. It is suggested that an additional term, Δu, accounting for the structural differences between tungsten ions should appear in the expression for the activation energy for the WO_3–$Na_2B_4O_7$ glasses such that

$$W = W_H + W_D/2 + \Delta u . \tag{12}$$

The density of states at the Fermi level can be estimated from the expression [24]

$$N(E_F) = 3/4\pi R^3 W . \tag{13}$$

The results for the present glasses are listed in Table 2. The values of $N(E_F)$ are reasonable for localized states.

The values of the small polaron coupling constant, γ_P, a measure of electron–phonon interaction, given by $\gamma_P = 2W_H/h\nu_0$ [21], were also evaluated for the present glasses. The estimated value of γ_P is 0.19–0.359 (Table 2), which is smaller than those for V_2O_5–Bi_2O_3 glasses doped with $BaTiO_3$ (7.05–7.60) [43] and CaO–BaO–Fe_2O_3–P_2O_5 glasses (21.0–29.2) [7]. A value of $\gamma_P < 4$ usually indicates weak electron–phonon interaction [24].

3.5 Nature of hopping conduction

The nature of polaron hopping, whether it is in the adiabatic or non-adiabatic regime, can be ascertained from a $\ln\sigma$ vs. W plot at fixed temperature T for glasses of different compositions [1, 5]. The estimated temperature, T_e, from the slope of such a plot will be close to T if the hopping is in the adiabatic regime (i.e. $\exp(-2\alpha R) = 1$ in Eq. (2)) and will be different from T if the hopping is in the non-adiabatic regime and the $\exp(-2\alpha R)$ term in Eq. (2) cannot ignored. The temperature T_e (in parentheses) is very different from the temperature at which $\ln\sigma$ is plotted against W in Fig. 7. This further supports the assertion that the tunnelling term $\exp(-2\alpha R)$ in Eq. (2) cannot be ignored and the conduction in the present glasses is in the non-adiabatic regime.

Studies of barium borovanadate glasses [4] have shown that the tunnelling term cannot be neglected. Similarly from the above analysis it is clear that the tunnelling term in Eq. (2) cannot be neglected and the conduction in the glass systems in the present study takes place in the non-adiabatic regime.

Similarly, to confirm the nature of hopping conduction (adiabatic or non-adiabatic) another method suggested by Holstein [11] is applied. He has suggested that SPH conduction at temperatures above $\theta_D/2$ can be discussed in terms of the polaron band width, J, expressed by [1, 11, 45]

$$J > \left(\frac{2kTW_H}{\pi}\right)^{1/4}\left(\frac{\hbar\nu_0}{\pi}\right)^{1/2} \quad \text{(adiabatic)} \tag{14}$$

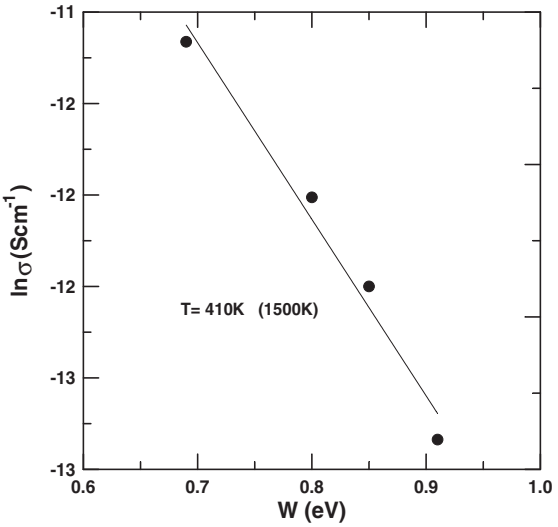

Fig. 7 Effect of activation energy, W, on dc conductivity, σ, at $T = 410$ K for different glass compositions.

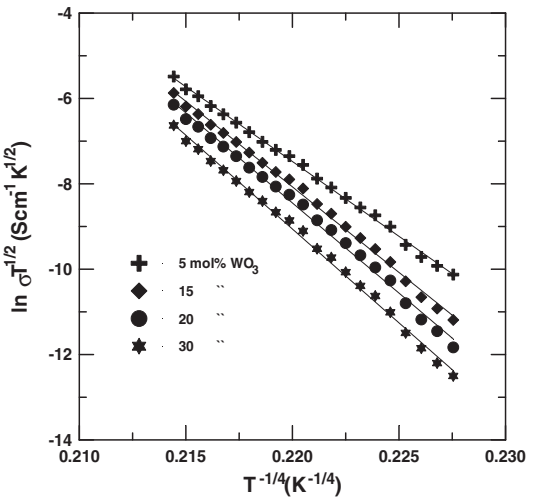

Fig. 8 Relation between ln $\sigma T^{1/2}$ and $T^{-1/4}$ for different glass compositions. The solid lines are calculated using the least-squares technique.

and

$$J < \left(\frac{2kTW_{\mathrm{H}}}{\pi}\right)^{1/4}\left(\frac{\hbar\nu_0}{\pi}\right)^{1/2} \quad \text{(non-adiabatic)} . \tag{15}$$

The polaron bandwidth can estimated from [23]

$$J \approx e^3[N(E_{\mathrm{F}})]^{1/2}/\varepsilon_{\mathrm{P}}{}^{3/2} . \tag{16}$$

Using a previous estimated value of $N(E_{\mathrm{F}})$ (Table 2), Eq. (16) gives $J \approx 0.003$ eV. The value of the right-hand side of Eq. (14) at 400 K is about 0.016 eV (Table 2). The values of the right-hand side of Eq. (14) for all the glass samples studied here are greater than the value of J suggesting that the hopping conduction is non-adiabatic in nature.

3.6 Variable-range hopping model

Mott [5] has given an expression for VRH at low temperatures; however, the samples under study are too resistive to enable measurement at low temperatures. Therefore Mott's VRH model could not be applied. Greaves [10] has suggested that VRH may dominate even at intermediate temperatures and has suggested another relation

$$\sigma T^{1/2} = A \exp\left(-B/T^{1/4}\right) \tag{17}$$

where A and B are constants and B is expressed by

$$B = 2.1[\alpha^3/kN(E_{\mathrm{F}})]^{1/4} . \tag{18}$$

Plots of ln $\sigma T^{1/2}$ vs. $T^{-1/4}$ are shown in Fig. 8 for four compositions of WO_3–$Na_2B_4O_7$ glass systems. These plots are linear in the range 363 to 468 K which suggests that Greaves's VRH model may be valid in these glasses over this temperature range. Using the slope obtained from this linear relation and the value of $N(E_{\mathrm{F}})$ given in Table 2 we can apply Eq. (18) to calculate the factor α. These values of α and $N(E_{\mathrm{F}})$ are reasonable for localized states [5, 23].

4 Conclusions

Semiconducting WO_3–$Na_2B_4O_7$ glasses were prepared by the press quenching technique from melts and the dc conduction mechanism was investigated in terms of different physical models. The density and molar volume for these glasses are consistent with the ionic size, atomic weight and amount of different elements in the glasses. At high temperatures the Mott model of phonon-assisted small polaron hopping between nearest neighbours is consistent with conductivity data, while at intermediate temperatures the Greaves variable-range hopping model is found to be appropriate. The electrical conduction in the high-temperature regime (temperature higher than half the Debye temperature θ_D) was confirmed to be due to non-adiabatic small polaron hopping of electrons between tungsten ions. The W–W ion spacing, R, evaluated as 4.07–4.39 Å, decreases with increasing WO_3 content. The values of α and $N(E_F)$ are reasonable for localized states.

References

[1] M. Sayer and A. Mansingh, Phys. Rev. B **6**, 4629 (1972).
[2] L. Murawski, C. H. Chung, and J. D. Mackenzie, J. Non-Cryst. Solids **32**, 91 (1979).
[3] M. M. El-Desoky, M. Y. Hassaan, and M. H. El- Kottamy, J. Mater. Sci., Mater. Electron. **9**, 447 (1999).
[4] M. M. El-Desoky, phys. stat. sol. (a) **195**, 422 (2003).
[5] N. F. Mott, J. Non-Cryst. Solids **1**, 1 (1968).
[6] I. G. Austin and N. F. Mott, Adv. Phys. **18**, 41 (1969).
[7] M. M. El-desoky and I. Kashif, phys. stat. sol. (a) **194**, 89 (2002).
[8] S. Sen and A. Ghosh, Phys. Rev. B **60**, 15143 (1999).
[9] N. F. Mott, Philos. Mag. **19**, 835 (1969).
[10] G. N. Greaves, J. Non-Cryst. Solids **11**, 727 (1973).
[11] T. Holstein, Ann. Phys. (NY) **8**, 325 (1959).
[12] J. Schnakenberg, phys. stat. sol. (a) **28**, 623 (1968).
[13] D. Emin, Adv. Phys. **24**, 305 (1975).
[14] D. Emin, Phys. Rev. Lett. **32**, 303 (1974).
[15] E. Gorham and D. Emin, Phys. Rev. B **15**, 3667 (1977).
[16] A. A. Bahgat and Y. M. Abou-zeid, Phys. Chem. Glasses **42**, 361 (2001).
[17] M. M. El-Desoky, K. Tahoon, and M. Y. Hassaan, Mater. Chem. Phys. **69**, 180 (2001).
[18] A. Ghosh and B. K. Chaudhuri, J. Non-Cryst. Solids **83**, 151 (1986).
[19] M. M. El-Desoky, J. Phys. Chem. Solids **59**, 1659 (1998).
[20] P. S. Tarsikka and B. S. Singh, J. Non-Cryst. Solids **124**, 221 (1990).
[21] N. F. Mott, Adv. Phys. **16**, 49 (1967).
[22] H. Hirashima, D. Arai, and T. Yoshida, J. Am. Ceram. Soc. **68**, 486 (1985).
[23] K. Sega, Y. Kuroda, and H. Sakata, J. Mater. Sci. **33**, 1303 (1998).
[24] N. F. Mott and E. A. Davis, Electronic Processes in Non-Crystalline Materials (Clarendon, Oxford, 1979).
[25] H. H. Qiu, H. Mori, H. Sakata, and T. Hirayama, J. Ceram. Soc. Japan **103**, 32 (1995).
[26] D. Deal, M. Burd, and R. Brunstein, J. Non-Cryst. Solids **54**, 207 (1983).
[27] H. Hirashima, H. Kurokawa, K. Mizobuchi, and T. Yoshida, Glastech. Ber. **61**, 151 (1988).
[28] M. M. El-Desoky, J. Mater. Sci., Mater. Electron. **14**, 215 (2003).
[29] L. Friedman and T. Holstein, Ann. Phys. **21**, 494 (1963).
[30] M. B. Field, J. Appl. Phys. **40**, 2628 (1969).
[31] H. Nasu, K. Hirao, and N. Soga, J. Am. Ceram Soc. **64**, C63 (1981).
[32] M. M. El-Desoky, H. Farouk, A. M. Abdalla, and M. Y. Hassaan, J. Mater. Sci., Mater. Electron. **9**, 77 (1998).
[33] A. Mansingh, A. Dhawan, R. P. Tandon, and J. K. Vaid, J. Non-Cryst. Solids **27**, 309 (1978).
[34] H. Mori, T. Kitami, and H. Sakata, J. Non-Cryst. Solids **168**, 157 (1994).
[35] H. H. Qiu, M. Kudo, and H. Sakata, Mater. Chem. Phys. **51**, 233 (1997).
[36] H. Sakata, K. Sega, and B. K. Chaudhuri, Phys. Rev. B **5**, 2330 (1999).
[37] H. Mori, H. Motsuno, and H. Sakata, J. Non-Cryst. Solids **276**, 78 (2000).
[38] M. Sayer and A. Mansingh, J. Non-Cryst. Solids **58**, 91 (1983).
[39] H. R. Killias, Phys. Lett. **20**, 5 (1966).

[40] I.G. Austin and E. S. Garbet, in: Electronic and Structural Properties of Amorphous Semiconductors, edited by P. G. Le Comber and J. Mort (Academic Press, New York, 1973), p. 393.
[41] M. Sayer, A. Mansingh, J. M. Reyes, and G. Rosenblatt, J. Appl. Phys. **42**, 2857 (1971).
[42] V. N. Bogomolov, E. K. Kudinov, and Yu. Firsov, Sov. Phys. Solid State **9**, 2502 (1968).
[43] A. Ghosh, J. Appl. Phys. **66**, 2425 (1989).
[44] A. Miller and E. Abrahams, Phys. Rev. **120**, 745 (1960).
[45] S. Muthupari, S. Lakshi Raghavav, and K. J. Rao, J. Phys. Chem. **100**, 4243 (1996).